

# **CHAPTER - IV**

**CHAPTER IV**  
**STUDIES ON PHOTOELECTROCHEMICAL (PEC) CELLS**  
**BASED ON PbS:CuS MIXED PHOTOELECTRODES**

4.1 Introduction	68
4.2 Electrochemistry of a Semiconductor / Electrolyte (S/E) Interface	68
4.2.1 Double layer at the interface	71
a) Electrolyte side of the interface	
b) Semiconductor side of the interface	
c) Effect of surface states and surface adsorbed ions	
4.2.2 Charge transfer at the S/E interface	80
a) In dark	
b) In light	
4.2.3 Some cell parameters	86
4.3 Experimental Procedure	87
4.3.1 Preparation of PbS and PbS:CuS photoelectrodes	87
4.3.2 Electrical characterisation of a PEC cell	88
4.3.3 Optical characterisation of a PEC cell	88
a) Photo response	
b) Speed of response	
4.4 Results and Discussion	89
4.4.1 Electrical properties	90
a) Current-Voltage characteristics in dark	
b) Capacitance-Voltage characteristics in dark	
c) Power output characteristics in light	

4.4.2 Optical properties	97
a) Photoresponse	
b) Speed of response	
4.5 Conclusions	101
References	102

#### 4.1 Introduction

Although semiconductor/electrolyte junctions are extremely simple and most convenient to fabricate, their properties are closely related to the properties of the semiconductor photoelectrode. Therefore it is necessary to know the prehistory of the photoelectrode material. The photoelectrochemical behaviour of the material changes drastically with its properties, especially the impediment of the charge carriers across the interface and generation of the photocurrent and photovoltage in a cell are dependent on the properties of the semiconductor electrode. Thus it is essential to understand the impact of various material properties on the photoelectrochemical performance of the material itself. The material properties such as structural, electrical and optical those decide its use as active photoelectrodes in a PEC cell are discussed in chapter III. The relevant theoretical background on the electrochemistry of electrode/electrolyte interface is given in section 4.2. Section 4.3 points out the minimum experimental know how's for devising the photoelectrochemical cell.

#### 4.2 Electrochemistry of Semiconductor/Electrolyte (S/E) Interface

The charge transfer across the S/E interface in dark or in light results in the flow of current through the junction. This is the key concept for working in the photoelectrochemical solar cell and reports are now available those throw some light on the analogy between the semiconductor and electrolyte as /1,2/: i) the oxidised and reduced species are analogous to the conduction and valance bands, respectively, ii) a term  $E_{F_{red/ox}}$  can also be defined similar to a semiconductor Fermi level  $E_F$ , iii) the

energy necessary to transfer an electron from the reduced species to the oxidised species is analogous to the band gap,  $E_g$ , of a semiconductor and iv) redox potential is a potential required to transfer an electron from a redox species to a vacuum level or vice versa. This analogy seems to be imperfect in the sense that:

- i) the nature of the charge carriers in the two phases is entirely different, one is electronic while other is ionic,
- ii) In the semiconductors the environment seen by an electron is an electron cloud and its motion is under the periodic potentials of the positively charged and fixed ion cores. In electrolytes, ions move with an ionic cloud of opposite charge with or without change in solvation shell,
- iii) as the two phases are distinctly different it would be interesting to know what happens when the two are brought in contact. Deep inside the semiconductor, the charge carriers are under the isotropic forces and that inside the electrolyte net force on an ion is zero. Hence at the interface boundary, picture is different. At the interface an ion is under the two different forces; one due to ions of the electrolyte and other due to the electrons of the semiconductor electrode. This anisotropy of the forces at the boundary leads to a quite distinct structure of the interface compared to the bulk structure. These anisotropic forces result in a new arrangement of the solvent dipoles and ions of the electrolyte and electrons of the electrode. This electrification of the electrode/electrolyte interface is shown in figure 4.1. In the beginning, anisotropy of the forces at the interface makes the charge carriers to accumulate near the surface. When there is a

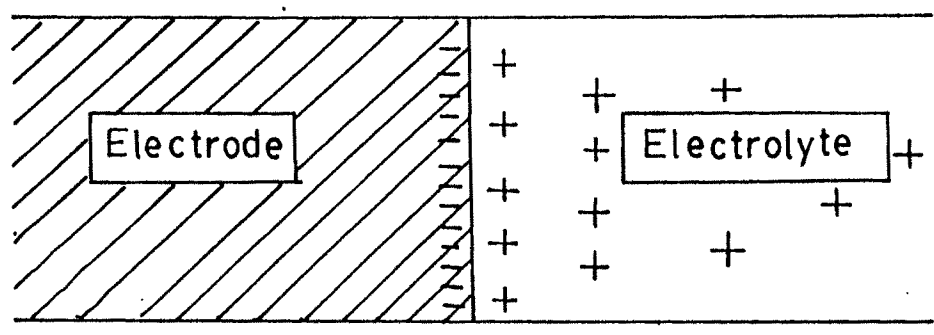
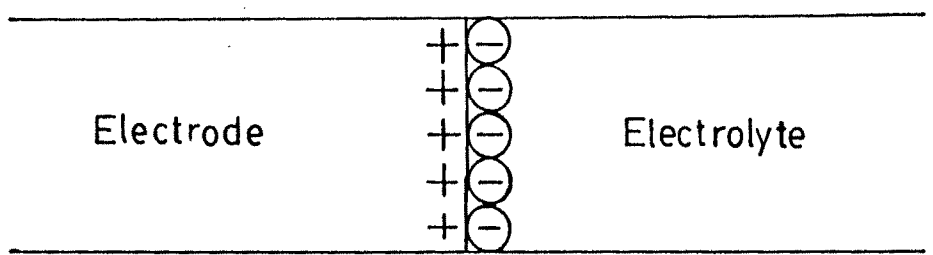
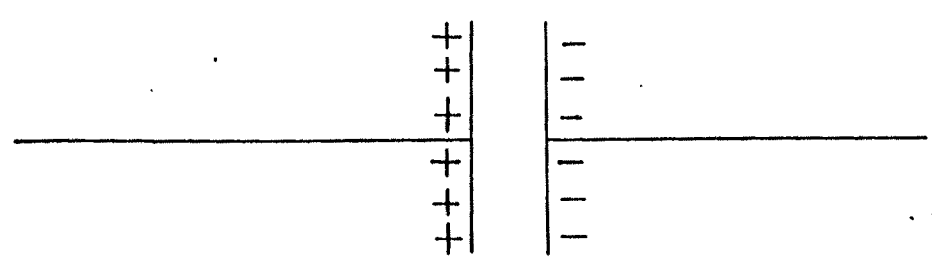


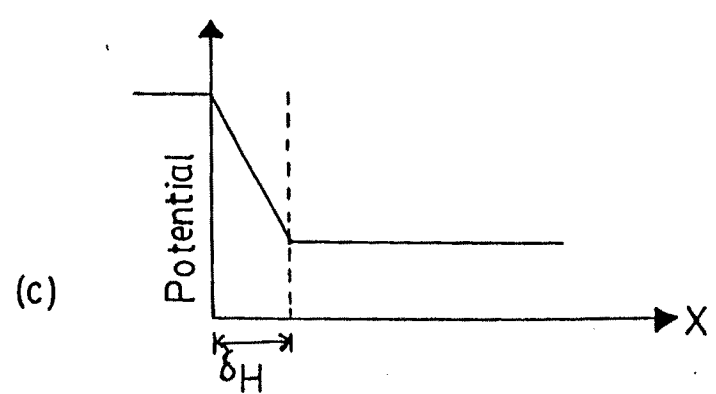
Fig.4.1 Qualitative description of charge distribution near the electrode/electrolyte interface.



(a)



(b)



(c)

Fig 4.2 Helmholtz-Perin model :  
 a) Schematic charge distribution  
 b) Electrical equivalent of interface  
 c) Potential distribution towards the electrolyte.

sufficient build up of charges on both sides the electrical forces at the surface overpower the barrier resulting in to flow of the charges. This potential gradient at the interface region acts as a barrier for further flow of the charges. The potential gradient is high at the surface and gradually decreases as we move away from it. This give rise to formation of a double layer.

#### 4.2.1 Double layer at the interface

The redistribution of the charges near the interface results into the rectification of the electrode/ electrolyte interface. At the interface charge neutrality occurs as;

$$q_s = q_{el} \quad \dots(4.1)$$

where,  $q_s$  and  $q_{el}$  are charges near the semiconductor and electrolyte sides of the interface, respectively. To examine the structure of a double layer we divide the interface into two regions: a) electrolyte side of the interface and b) electrode side of the interface.

##### a) Electrolyte side of the interface

Helmholtz/3/ assumed that the charged layers of the ions form a sheath at the dipped metal surface as shown in the figure 4.2(a). The Helmholtz-Perrin model suggests the electrode-electrolyte interface as a parallel plates of a condenser charged oppositely as shown in figure 4.2(b). The term double layer thus originated and all the potential is assumed to be dropped across this double layer of thickness  $\delta H$ . Initially,  $\delta H$  was assumed to be independent of the applied voltage and if the charge on the capacitor is  $dQ$  and potential across the layer is  $dV$  then the differential capacitor is given by;

$$C = \frac{dQ}{dV} = \frac{\epsilon \epsilon_0}{\int H} \left[ \text{where } \int H = \epsilon \epsilon_0 \frac{dV}{dQ} \right] \quad \dots(4.2)$$

where,  $\epsilon$  and  $\epsilon_0$  are the dielectric constants of the material and free space, respectively. Gouy /4/ and Chapman /5/ suggested that the electrode surface on which charges have accumulated forms a diffused layer called as "Gouy Layer" and the differential capacity of this Gouy Layer is voltage and concentration dependent. It was Stern who pointed out that the double layer is neither abrupt nor diffused but a combination of the two /6-9/ wherein the interface distribution is divided into two layers :

i) Dense : Here ions stuck to the electrode and potential variation is linear. ii) Diffused : Formed as a result of opposing tendencies of the attractive coulombic force and disordering thermal fluctuations where potential decays exponentially. These layers are shown in figure 4.3 (a,b).

The Stern model does not explain explicitly how the ions are stuck to the electrode. The probable reason may be the hydrated electrode surface and stripping OFF the solution. Here the water molecules are stripped OFF from the electrode surface and ions sit in close contact with the electrode. The ions so sitting are called contact adsorbed ions. The locus of all such ions form the "Inner Helmholtz Plane (IHP). The solvated ions from the Outer Helmholtz Plane (OHP). The situation is shown in figure 4.4. Recently Liu /9/ has developed a lattice gas model where both ions and solvent molecules are taken as hard spheres of equal radii forming a parallel layers near the planar electrode. The lattice parameter is chosen as the distance of closest approach. This model gave a reasonable description of the properties of the

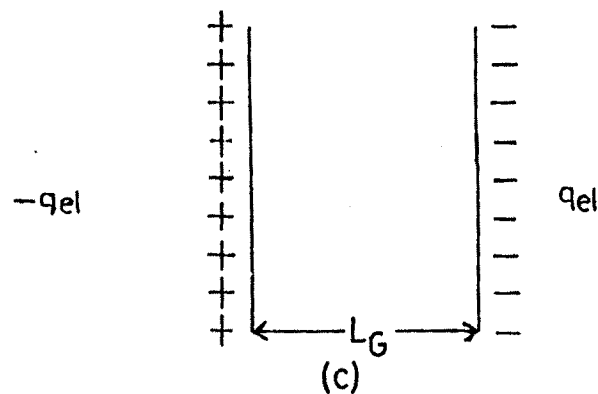
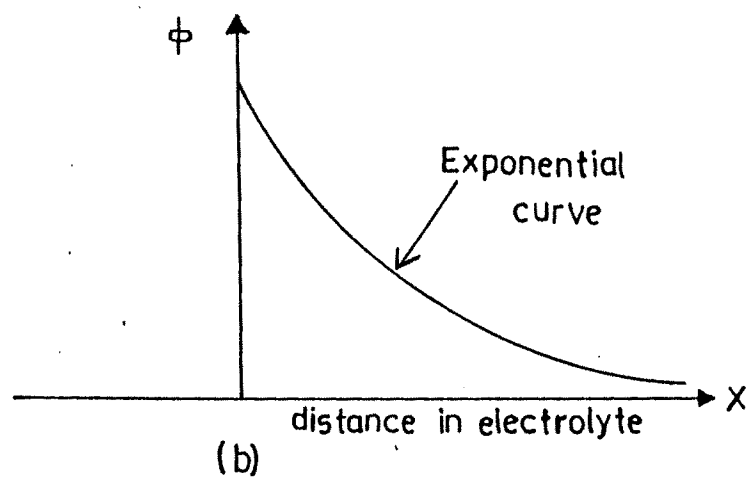
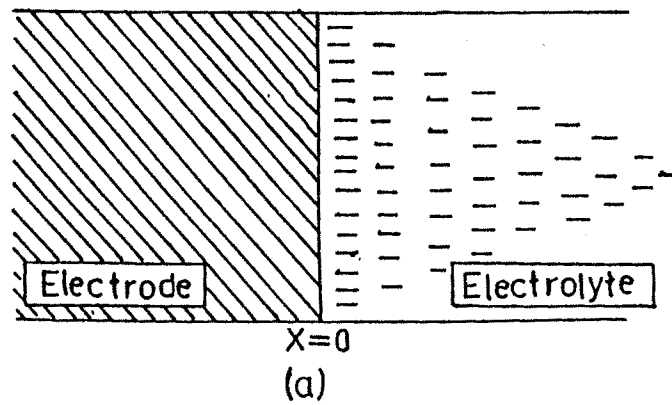


Fig. 4.3 Gouy - Chapman model :

- a) Schematic charge distribution
- b) Potential distribution in the electrolyte
- c) Simulated electrical equivalent.

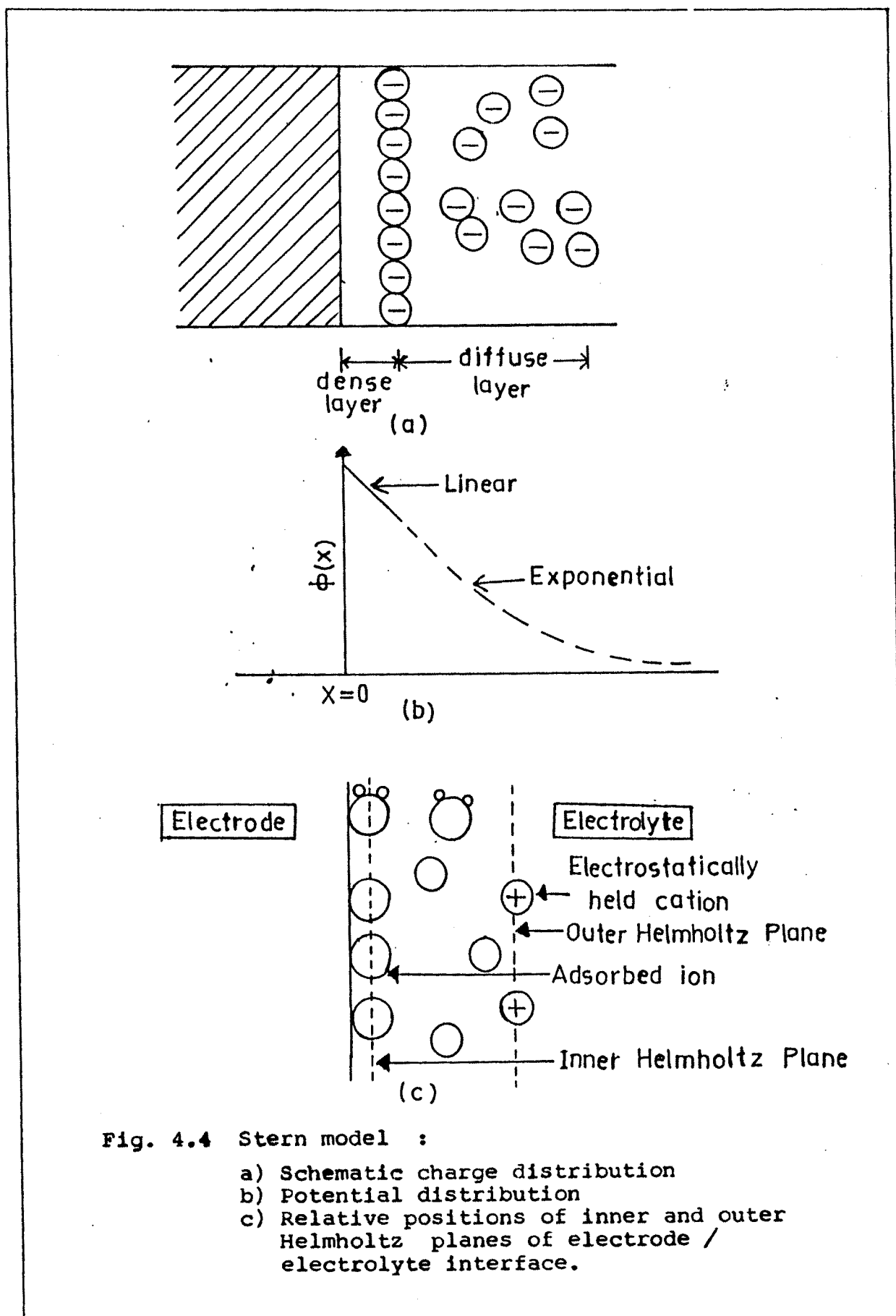


Fig. 4.4 Stern model :

- Schematic charge distribution
- Potential distribution
- Relative positions of inner and outer Helmholtz planes of electrode / electrolyte interface.

electrolyte in the interface region and is better than all the earlier models.

#### b) Semiconductor side of the interface

The first systematic investigation of the semiconductor/electrolyte interface was reported by Brittain and Garret /7/. A large number of references are now available with excellent aspects of semiconductor electrochemistry /1,6,8,9/. The charge distribution on the electrode side is widely different for metals and semiconductors principally because; i) Electrons and holes are the charge carriers in semiconductors while in metals only electrons carries the charge, ii) Carrier density in the semiconductors is  $10^{16}$  to  $10^{23}$   $\text{cm}^{-3}$  while for metals it is  $10^{28}$   $\text{cm}^{-3}$ ; iii) For metals, the charges are located at the surface while for semiconductors they form a space charge layer within the semiconductor near the interface.

The potential and charge distribution on the electrode side of the S/E and M/E interfaces are given in figure 4.5 (a,b). The nature of the space charge layer depends upon the manner in which charge transfer occur across the interface. Three types of situations arise; i) If a semiconductor acquires excess majority carriers, the space charge layer is termed an "enrichment layer". Such a layer leads a downward band bending for n-type while upward for p-type semiconductors, ii) If surface becomes depleted of majority carriers then space charge is known as "depletion layer". This leads to the upward band bending for p-type semiconductors, iii) If the charge distribution is such that the minority carrier concentration at the surface is greater than

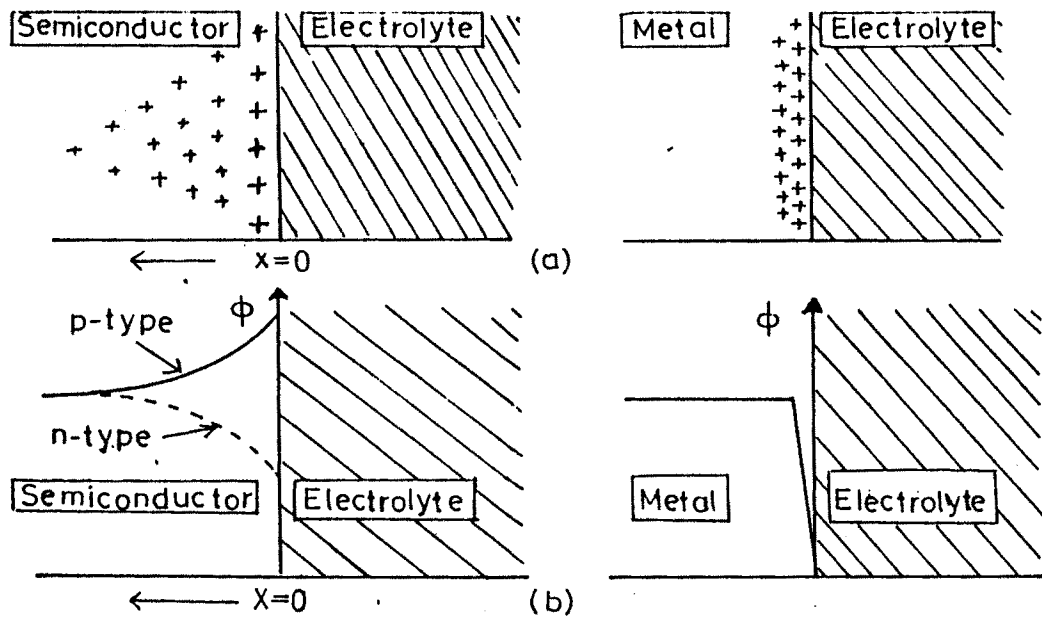


Fig.4.5 Difference between metal/electrolyte and semiconductor/electrolyte interface :  
 a) Charge distribution    b) Potential distribution

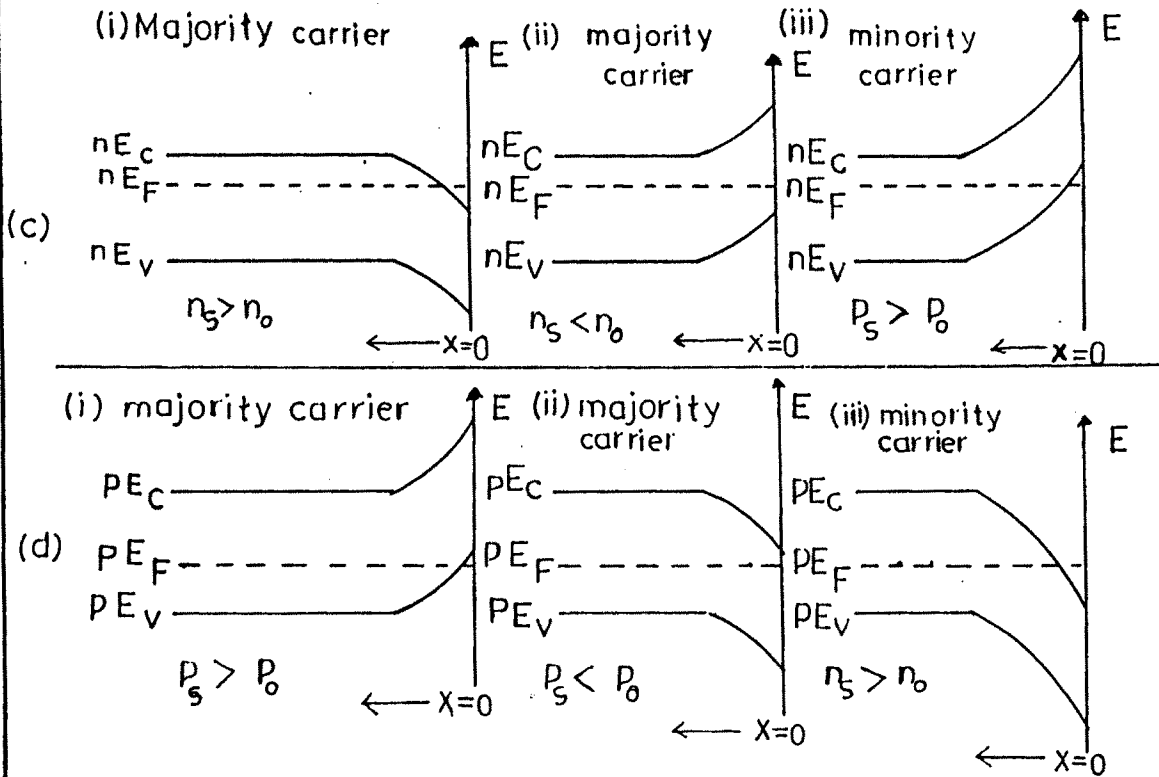


Fig.4.5 Three types of space charge layers namely enrichment, depletion and inversion at :  
 c) n - type semiconductor  
 d) p - type semiconductor

that within the bulk. Space charge layer under this condition is called as an "inversion layer". This leads to a large upward band bending for n-type and downward for p-type. The above three situations are shown in figure 4.5 (c,d).

**c) Effect of surface states and surface adsorbed ions**

The potential and charge distribution at the electrode/electrolyte interface are affected by the presence of surface states and surface adsorbed ions. Surface states are essentially the results of non-periodicity of the lattice at the boundary and adsorption of the foreign atoms or ions at the interface and acts as the traps for charge carriers and hence substantially modify the space charge. Thus resulting picture of the semiconductor/electrolyte interface consists of; i) diffused space charge layer in the semiconductor including surface states and surface adsorbed ions, ii) Helmholtz layer and iii) Gouy layer.

**d) Differential capacitance and Mott-Schottky plot**

The simplest electrical equivalent of a S/E interface can be regarded as a series combination of three capacitances  $C_{SC}$ ,  $C_H$  and  $C_G$ . Hence the total capacitance is given by /9/;

$$\frac{1}{C_T} = \frac{1}{C_{SC}} + \frac{1}{C_H} + \frac{1}{C_G} \quad \dots(4.3)$$

where,  $C_{SC}$  is the space charge capacitance,  $C_H$  and  $C_G$  are the Helmholtz and Gouy layer capacitances, respectively. For PEC cells the total capacitance is solely that due to a space charge layer and the surface states deteriorate the performance of a PEC cell. Therefore a model to account for the behaviour of surface

states can be incorporated in the interface as shown in figure 4.6 /7,9/. Each of the  $n$  surface states is represented as a series combination of a capacitance ( $C$ ) and a resistor ( $R$ ). The surface states are in parallel with each other and with the semiconductor space charge capacitance ( $C_{SC}$ ). The total electrode capacitance therefore, is  $C_{SC} = \sum C_i$ . This network of parallel capacitances is in series with the bulk resistance ( $R_S$ ) of the material, the double layer capacitance ( $C_{DL}$ ) and the solution resistance ( $R_{sol}$ ) between the semiconductor and the reference electrode. Any Faradic process will short across  $C_{SC}$  and  $C_{DL}$  as represented by  $Z$ . The Faradaic process can be minimized by making  $Z$  infinite. Also  $C_{DL} \gg C_{SC}$  and can be ignored /7,9/. The measurement of a differential space charge layer capacitance provides a convenient tool to analyse a S/E interface and for obtaining the useful informations about both the semiconductor and an electrolyte. Neglecting the surface states and assuming all the donors and acceptors as fully ionised and high ionic concentration of the redox couple, the space charge layer capacitance is given by;

$$C_{SC}^{-2} = \frac{2}{\epsilon_s \epsilon_0 q N_D} \left( V - V_{fb} - \frac{KT}{q} \right) \quad \dots(4.4)$$

where,  $\epsilon_s$  is the dielectric constant of the semiconductor,  $\epsilon_0$  is the permittivity of the free space,  $V$  is the applied electrode potential and  $V_{fb}$  is the flat band potential. Equation (4.4) is a famous Mott-Schottky equation according to which a plot of  $C_{SC}^{-2}$  vs  $V$  will be a straight line and intercept on voltage axis gives the value of ' $V_{fb}$ ' and the slope gives the donor concentration. The diagrammatic representation is shown for  $n$  and  $p$  type

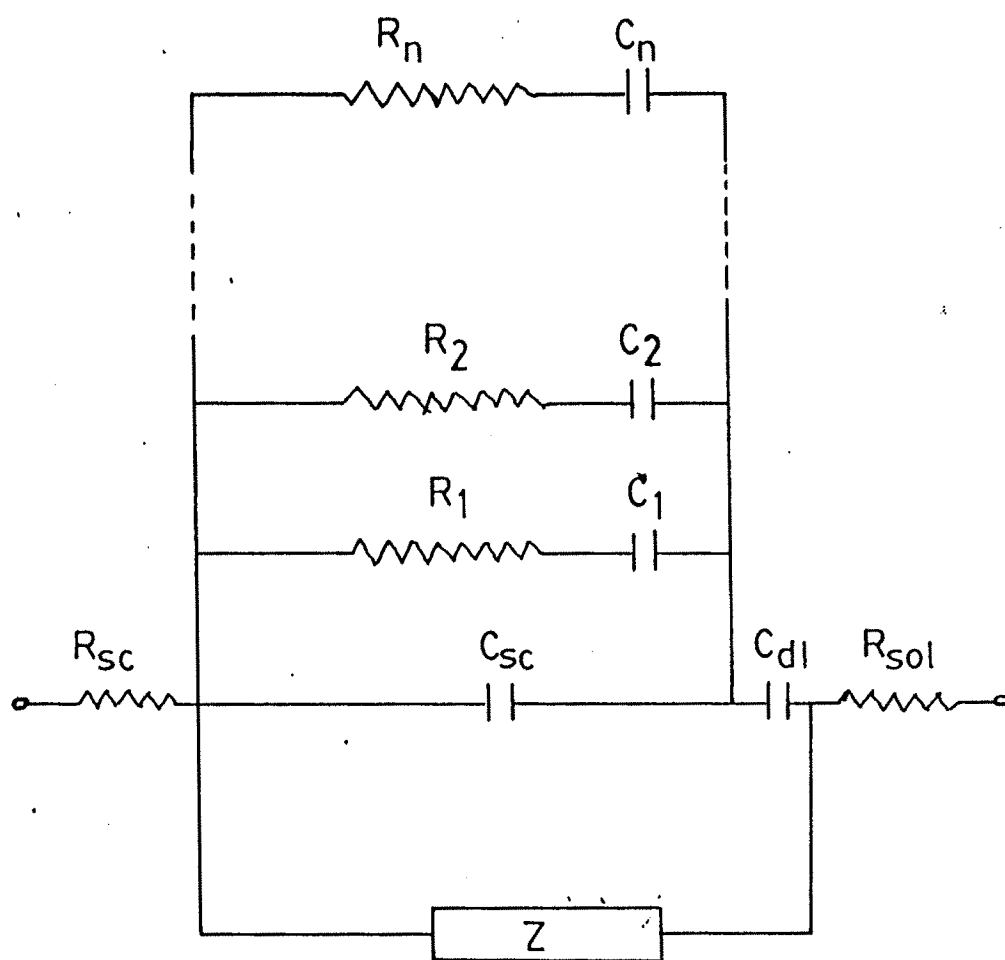


Fig. 4.6 An equivalent circuit for the semiconductor/electrolyte interface.

semiconductors in figure 4.7. Further the Mott-Schottky plot determines the type of majority carriers and the band bending which is a maximum open circuit voltage that can be obtained from a PEC cell.

The ideal Mott-Schottky behaviour is more an exception than a rule for the semiconductor electrolyte interface. The departure from an ideal behaviour is observed for many semiconductors /9-12/. Some of the reasons for this non-ideality are; i) geometrical factors such as the edge effect, non-planar interface, surface roughness etc leading to non-uniform a.c current distribution, ii) non-uniform doping, iii) presence of both donor and acceptor impurities, iv) presence of deep donors and acceptors and v) an extra contribution  $C^i$  to the total capacitance due to; a) the presence of an oxide film, b) ionic adsorption on the surface, c) Helmholtz layer capacitance, d) existence of an acid-base equilibrium at the interface.

#### 4.2.2 Charge transfer at S/E interface

An electron may be transferred either from an electrolyte to the electrode and vice-versa under the suitable values of valance and conduction band energies and a proper choice of an electrolyte-redox couple. The ionic species will either be reduced or oxidised at the respective elctrodes.

##### a) In dark

To understand the charge transfer process across the electrode /elctrolyte interface in dark let us consider the motion of the ions from solution side to the electrode and back. There occurs both electronation,

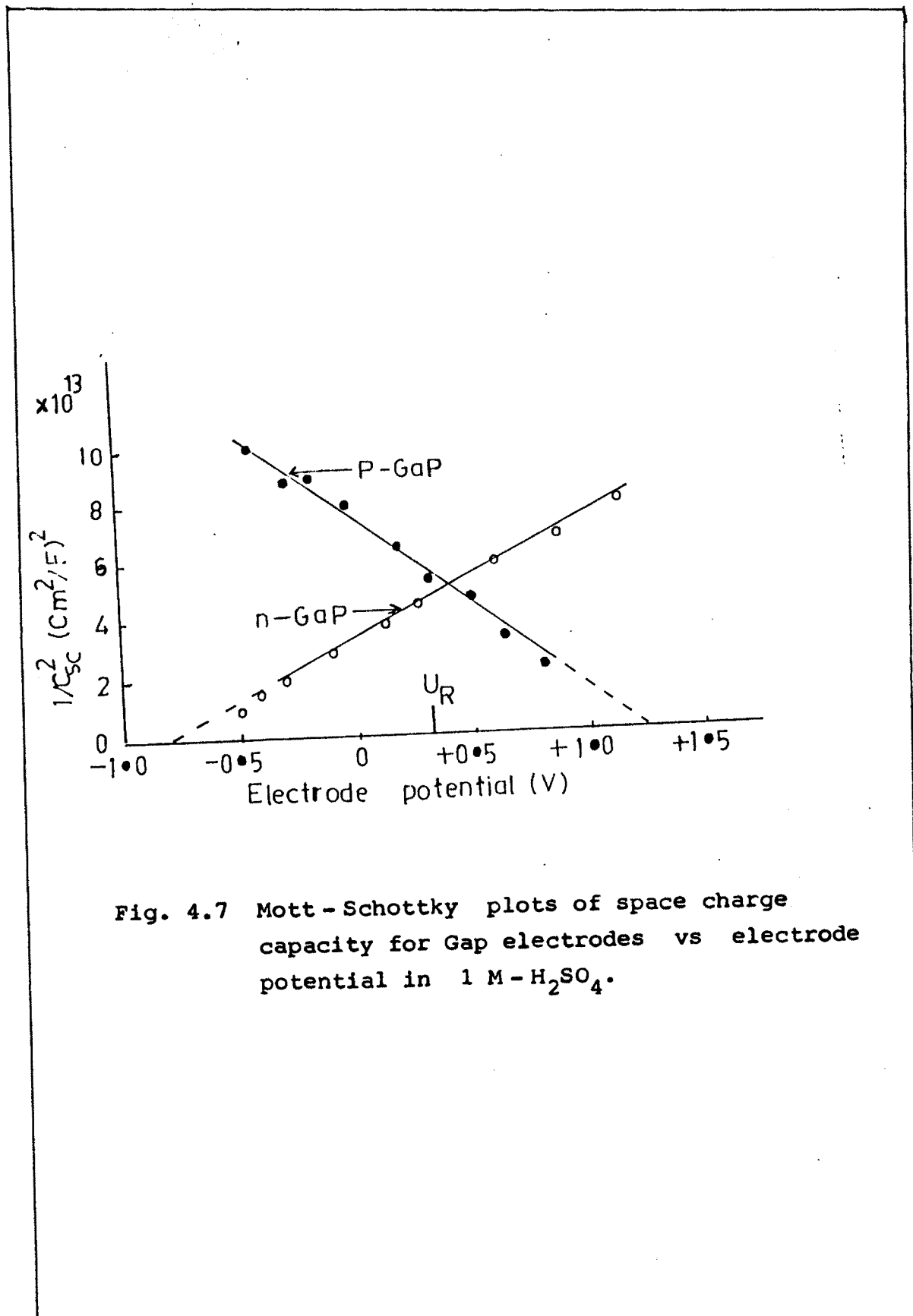
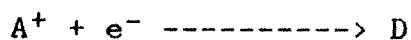
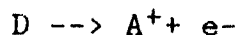


Fig. 4.7 Mott-Schottky plots of space charge capacity for GaP electrodes vs electrode potential in 1 M-H<sub>2</sub>SO<sub>4</sub>.



and deelectronation



reactions /6,7,9 /.

If a positive ion moves against the field direction in an electronation reaction, it moves in the direction of field in de-electronation reaction. This is shown in figure 4.8(a). Further if the positive ion has to be activated through a potential difference ' $B\Delta\phi$ ' in electronation reaction, it has to be activated through the remainder  $(1 - B\Delta\phi)$  in de-electronation reaction where B is the symmetry factor and  $\phi$  is a potential through which ion passes. Therefore the rates of electronation and de-electronation reactions and respective current densities and their difference can be evaluated.

We can then write the net current density as :

$$i = i_0 \left[ \exp \left( (1-B) \frac{VF}{RT} \right) - \exp \left( - \frac{BVF}{RT} \right) \right] \quad \dots(4.5)$$

Equation (4.5) is the famous Butler - Volmer relation /6,9/ and shows dependence of the current density through a metal - solution interface on the potential V. Small changes in V produce large changes in i. In the electrode / electrolyte system there is a hill shaped barrier even in the absence of an electric field as shown in figure 4.8(b)

#### b) In light

Upon illumination the photogenerated carriers in the depletion region are separated by an electric field at the interface /13,14/. The charge separation process results in a counter field which is maximum at the open circuit condition

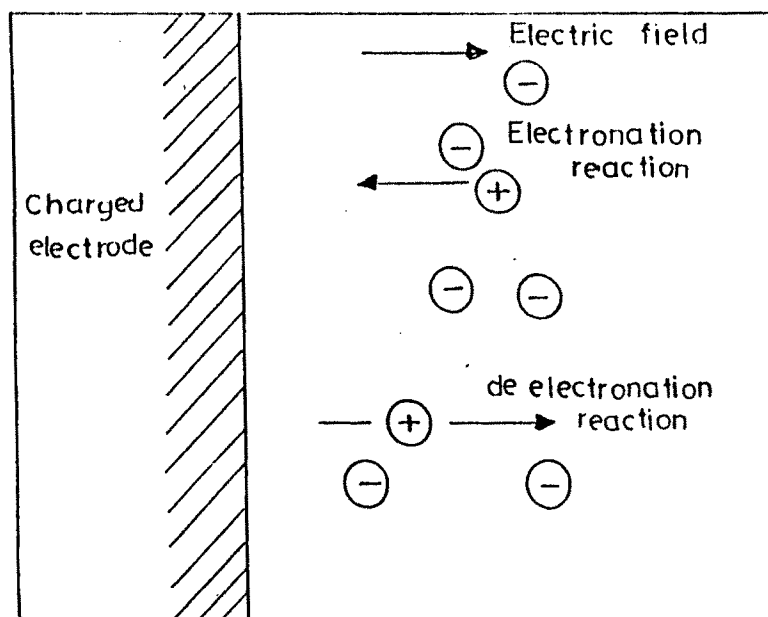


Fig. 4.8(a) Electric field effect on electronation de-electronation reactions.

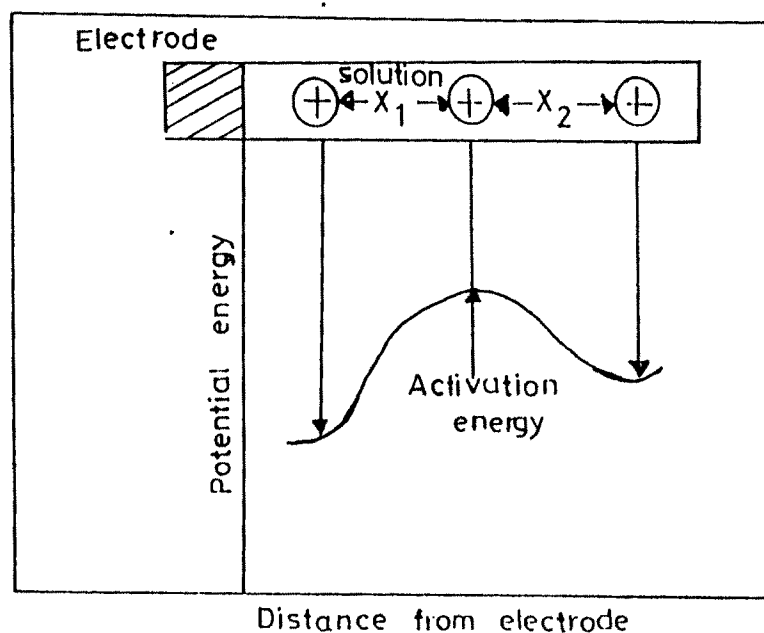
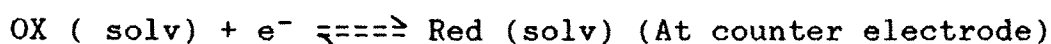
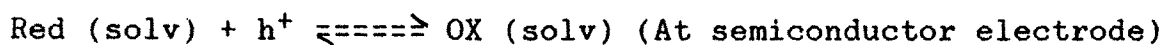


Fig. 4.8(b) Construction of a potential energy distance profile by consideration of the potential energy change produced by varying  $X_1$  and  $X_2$ .

called as  $V_{oc}$ . This photovoltage drags the electrons from semiconductor to the counter electrode where as electrolyte captures the holes. The reaction as a whole can be formulated as;



The electrode plays nothing in the reaction but acts only as a shuttle for charge transfer mechanism. Consider a n-type semiconductor in contact with an electrolyte under illumination and with a forward voltage  $V$  applied. The schematic showing the energy level diagram of electron is shown in figure 4.9. The quasi-Fermi levels for electrons ( $E_{Fn}$ ) and for holes ( $E_{Fp}$ ) in the depletion region are assumed flat. If  $U$  is the separation between them then,

$$E_{Fn} - E_{Fp} = qU \quad \dots(4.6)$$

The assumption that  $U > V$  represents the fact that minority carrier concentration under illumination is larger than its concentration in dark. For hole flux to flow from the semiconductor to electrolyte,  $U$  is defined as

$$\exp \frac{qU}{KT} = P(W) / P_0 \quad \dots(4.7)$$

where,  $P(W)$  is the hole concentration at the edge of the depletion region ( $X = W$ ) and  $P_0$  is the equilibrium hole concentration in the bulk of the semiconductor in dark. Most of the applied voltage appears across the semiconductor depletion region thus the series resistance of a cell should be negligible and an electrolyte concentration should be high enough such that

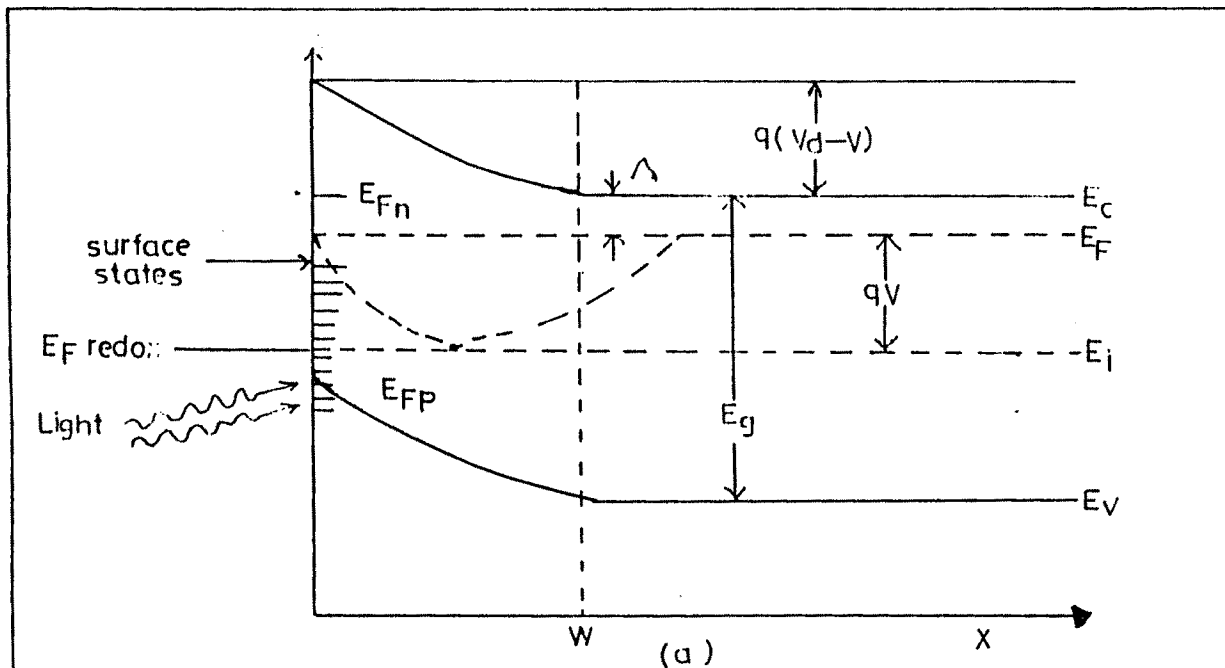


Fig. 4.9 Electron energy level diagram for n-type semiconductor photoelectrode near the S/E interface under illumination and forward bias  $V$  reducing the band bending from  $qV_D$  to  $q(V_D - V)$ .

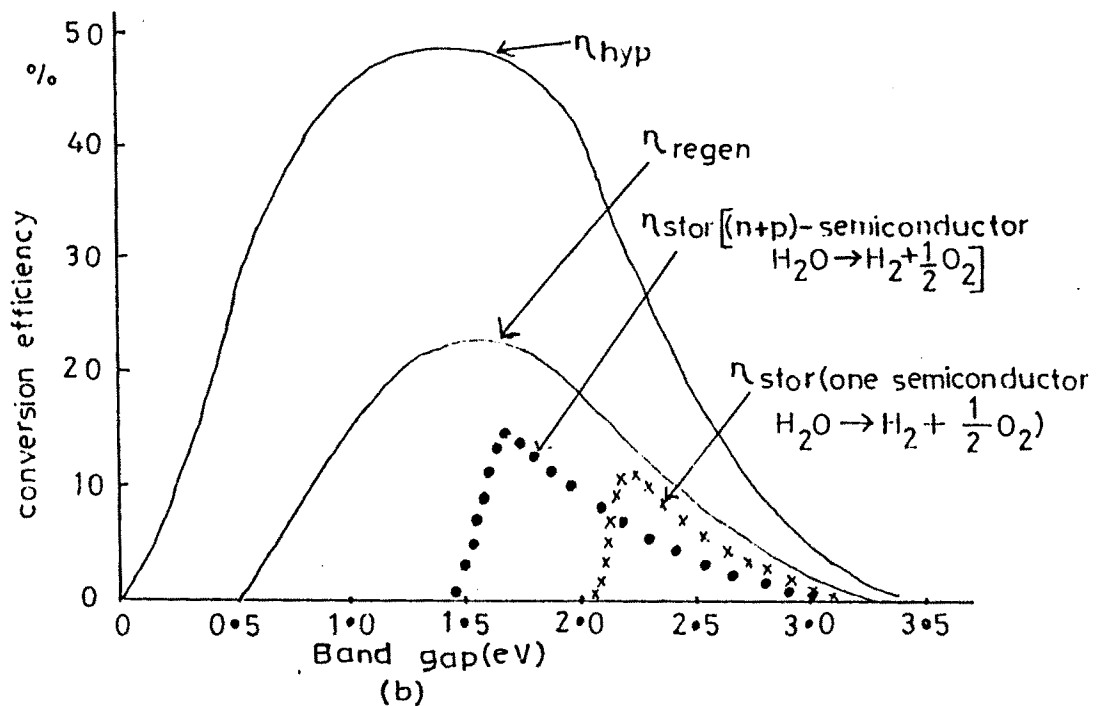


Fig. 4.10 Estimated optical conversion efficiencies of the PEC solar cells for power generation (regenerative cell)  $\eta_{regen}$  and storage,  $\eta_{stor}$ .  $\eta_{hyp}$  is the theoretical energy conversion efficiency for AM<sub>1</sub> (Gerischer - 1979).

$C_H > C_{SC}$ . The depletion layer width under such circumstances is;

$$W = W_0 (V_D - V_0)^{1/2}$$

and

$$W_0 = \frac{(2 \epsilon_s \epsilon_0)}{qN_D} \quad \dots(4.8)$$

where,  $\epsilon_s$  is the dielectric constant of the material and  $\epsilon_0$  is the permittivity of the free space,  $N_D$  is the donor concentration and  $V_D$  is the equilibrium band bending voltage. If  $S_t$  is the surface transfer velocity,  $S_r$  is the surface recombination velocity,  $\theta_0$  is the incident photon flux,  $\alpha$  is the light absorption coefficient and  $W$  is the width of the depletion region, then the photo flux can be given as

$$j_l = \left( \frac{S_t}{S_r} \right) \theta_0 \left[ 1 - \exp \frac{(\alpha - W)}{1 + \alpha t} \right] \quad \dots(4.9)$$

This is the useful photogenerated current of a solar cell /7,9,14/ whose direction is from semiconductor to the electrolyte.

#### 4.2.3 Some cell parameters

The band bending characteristic of the semiconductors at the interface limits the output voltage / power and the maximum photopotential is obtained when the bands are almost flat. The conversion efficiency ( $\eta$ ) is given as,

$$\eta = \frac{(\text{Output power})}{(\text{Input power})} \times 100\% \quad \dots(4.10)$$

In actual the efficiency ( $\eta$ ) is given as /9,15/;

$$\eta = E_g \frac{\int_{E_g}^{\infty} \alpha(E) N(E) dE}{\int_0^{\infty} E \cdot N(E) dE} \dots(4.11)$$

(neglecting ohmic loss , over potential , light absorption in the solution.)

where,  $E_g$  = band gap of the material,  $N(E)$  = number of photons with energy  $E$ ,  $\alpha(E)$  = fraction of the photons absorbed.

Equation (4.11) is suggested for the large magnitudes of  $E_g$  and  $\alpha$ . Further  $\alpha(E)$  near the band edge is approximated as/9/;

$$\alpha = \frac{A(h\nu - E_g)^n}{h\nu} \dots(4.12)$$

where ,  $A$  = constant and  $n = 1/2$  for direct allowed and  $n=2$  for indirect transitions. Thus equation (4.11 ) and (4.12) are contradictory and  $n$  would be a maximum for some optimum value of  $E_g$  (1.2 eV) as shown in figure 4.10. From figure 4.9 it is clear that a theoretical efficiency of about 25% is expected for regenerative typ PEC cell. As the maximum open circuit voltage from a PEC cell depends on  $V_{redox}$  also , the ultimate conversion efficiency would also depend upon  $V_{redox} - V_{Fb}$ .

### 4.3 Experimental Procedure

#### 4.3.1 Preparation of PbS and PbS:CuS photoelectrodes

The PbS and PbS:CuS thin film photoelectrodes were deposited onto the mirror grade polished stainless steel substrates as described in section 2.2.4. A typical photoelectrochemical cell was constructed using one of these samples as a photoelectrode , a mixture of equimolar NaOH-S-Na<sub>2</sub>S as an electrolyte and CoS treated graphite rod as a counter

electrode.

#### 4.3.2 Electrical characterisation of a PEC cell

Design , fabrication and constructional details of a PEC cell are outlined in chapter II. The charge transfer mechanism across an electrode / electrolyte interface can be understood by examining the electrical and optical properties of a PEC cell. In view to achieve this , current - voltage and capacitance - voltage characteristics were studied . A potentiometric arrangement was employed to vary the potential across the junction and current through the junction was measured with a sensitive currentmeter. The same circuit was used to measure the space charge layer capacitance . The voltage across the junction was varied in a similar fashion as that of the previous and the junction capacitance was measured with an Aplab capacitance meter. The superimposed ac voltage was 1V pp. The reverse saturation current of the various cells was measured in the 30°C to 100°C temperature range for the calculation of the barrier heights . The power output characteristics were obtained under 40 mW/cm<sup>2</sup> intensity.

#### 4.3.3 Optical characterisation of a PEC cell

The optical characterisation of a PEC cell mainly involves the measurement of photoresponse and speed response.

##### a) Photoresponse

This is the measurement of a short circuit current (Isc) and a open circuit voltage (Voc) under various illumination intensities . The illumination was measured with a digital lux meter , L X - 101 and Isc and Voc were noted with the sensitive

current and volt meters, respectively.

#### c) Speed of response

It is a measurement of  $I_{sc}$  or  $V_{oc}$  with time under constant illumination. Thus  $V_{oc}$  was measured up to a steady state value for various time intervals and then illumination intensity was cut off and the decay in  $V_{oc}$  was also noted for different time intervals. Further cycles can be repeated.

#### 4.4 Results and Discussion

It is now clearly understood from the several experimental evidences that when a semiconductor photoelectrode is brought into contact with an electrolyte there occurs a drastic degradation in the performance of an electrochemical photovoltaic cell. This undesirable degradation will not allow the cell to yield the satisfactory results in a reproducible fashion. Further, it is the photoelectrode that governs almost all the properties of a photoelectrochemical cell which can be examined by examining the changes in its several thin film properties/9,16,17,18/. The film properties those govern the performance of a PEC cell are electrical conductivity, carrier mobility and concentration, thermoelectric power, activation energy, optical absorbance, mode of transition, grain dimension, nature of the material of the material (single or polycrystal) etc. These properties and their effectiveness have been described vis-a-vis in chapter III. It is now left for this chapter to observe their reflections via the cell properties. Therefore this chapter is fully devoted to the application part of PbS:CuS film photoelectrode in PEC cell. As the nature of contact between the substrate and the material plays an important role, it has been tested. It is found that

PbS:CuS offers an ohmic contact to stainless steel . The photoelectrochemical behaviour of PbS : CuS has been divided into two : i) the electrical studies and ii) the optical studies .

#### 4.4.1 The electrical studies

Electrical properties , particularly , current - voltage and capacitance - voltage characteristics in dark , power output curves in light and determination of barrier heights have been studied.

##### a) Current-Voltage characteristics in dark

A PEC cell has been formed with PbS:CuS as an active photoelectrode. It is seen that a dark voltage  $V_D$  and dark current  $I_D$  are generated in a cell. The dark voltage originates from the difference between two half cell potential in a PEC cell and can be given as

$$E = E_{\text{PbS:CuS}} - E_{\text{carbon}} \quad \dots(4.13)$$

where,  $E_{\text{PbS:CuS}}$  and  $E_{\text{carbon}}$  are half cell potentials developed when electrodes are dipped in the electrolyte. It is also observed that  $E_{\text{PbS:CuS}} < E_{\text{carbon}}$  and  $I_D$  is an indicative of some deterioration of the photoelectrode material. The dynamic I-V characteristics in dark have been studied at room temperature to understand the charge transfer process across the electrode/ electrolyte interface. Forward current is seen to increase rapidly with the applied voltage which can be ascribed to a small barrier height and increase in tunneling mechanism /9,16,17/. The reverse biased current deviates from the saturation because of the following reasons : i) the effective barrier height ( $\phi_B$ ) decreases because of the interfacial layer, ii) electron-hole

pairs are thermally generated in the depletion layer under high applied reverse bias and iii) The current increases due to the onset of an electron injection from the electrolyte into the semiconductor because the barrier becomes thin enough for tunneling to take place. The nature of the I-V curves can be understood from a Butler-Volmer relation as described in the section 4.4.2. The magnitude of the symmetry factor  $B$  is calculated from these observations and is found to be greater than 0.5 which shows that the junctions formed are of the rectifying type /6,19/ and analogous to the Schottky barrier junction /6,19/. This is called Faradaic rectification /16,19/. The quality of the junction can be decided in terms of a factor, so called junction ideality factor ( $n_d$ ) and therefore the junction quality factor in dark is determined from the variation of  $\log I$  Vs  $V$  plot for the various cells (figure 4.11). The actual determination of  $n_d$  is carried out from the high voltage linear region of the plots. The magnitudes of  $n_d$  are listed in Table 4.1 and are relatively larger than ideal value. The equilibrium reverse saturation current density ( $I_0$ ) can be obtained from the above plots by extrapolating the straight portion of the graph to the current axis. They are of the order of  $10^{-5}$  A/cm<sup>2</sup>. The higher magnitude of  $n_d$  for all the cells is an indicative of the non-ideal junction and this non-ideality of the dark I-V characteristic can be related to the recombination mechanism and series resistance effects /17,20,21/.

The built-in-potential also called as the barrier height ( $\phi_B$ ) is determined for all the cell configurations by measuring the reverse saturation current at various working temperatures in

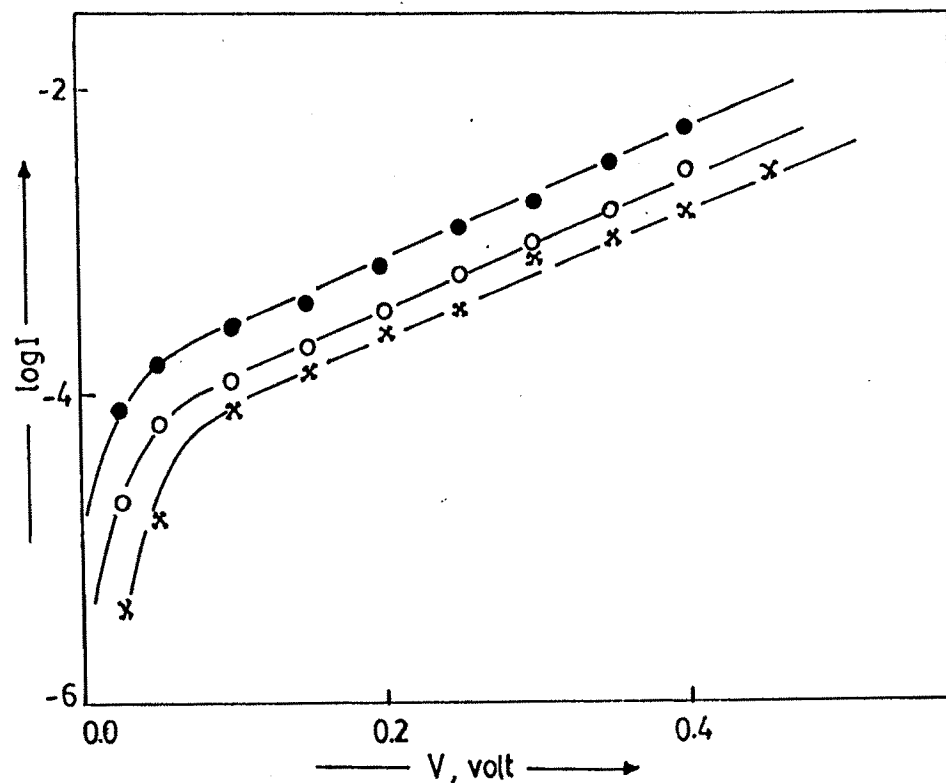


Fig.4.11 Variation of  $\log I$  vs  $V$  for the cells formed with different photoelectrodes.  
 $\circ \rightarrow$  Pure PbS,  $\bullet \rightarrow X = 0.05$ ,  $\times \rightarrow X = 0.075$

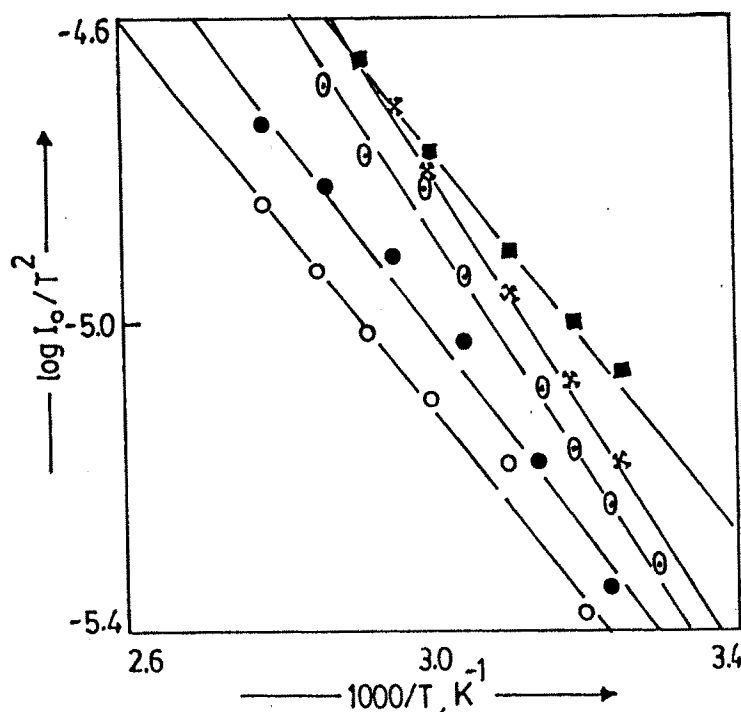


Fig.4.12 Determination of barrier height ( $\phi_B$ ) for various cell configuration.  $\circ \rightarrow$  pure PbS,  $\circ \rightarrow X = 0.05$ ,  
 $\bullet \rightarrow X = 0.075$ ,  $\times \rightarrow X = 0.35$ ,  $\blacksquare \rightarrow X = 0.5$ .

Table 4.1 Some parameters showing performance of PEC cells formed with PbS and PbS:CuS electrodes

Copper content	$I_{sc}$ (mA/cm <sup>2</sup> )	$V_{oc}$ (mV)	$\eta$ %	ff %	$R_s$ ohm	$R_{sh}$ ohm	$\phi_B$ (eV)	$n_d$	$V_{fb}$ Volts
0.0	0.15	58	0.00065	30.1	295	500	0.23	4.43	-0.21
0.05	0.26	130	0.0036	42.6	175	1850	0.31	4.21	-0.32
0.075	0.24	100	0.0016	26.3	340	300	0.26	4.64	-
0.15	0.215	125	0.0038	56.5	156	2000	0.33	4.30	-0.32
0.2	0.183	110	0.0027	-	-	-	-	-	-
0.35	0.160	97	0.0009	23.2	785	520	0.32	4.91	-0.28
0.5	0.183	95	0.0016	35.9	-	-	0.254	-	-0.24

the range from 30°C to 100°C. For a Schottky barrier junction the reverse saturation current ( $I_0$ ) is related to the built-in-potential ( $\phi_B$ ) as /21,22,23/;

$$I_0 = AT^2 \exp (- \phi_B / KT) \quad \dots(4.14)$$

where, A is the Richardson's constant and other symbols have their usual meaning. It has been seen that the reverse saturation current vary exponentially with temperature. Figure 4.12 depicts the variation of  $\log (I_0/ T^2)$  vs  $1/T$  for five typical cell configurations and the built-in-potentials ' $\phi_B$ 's have been determined from the slope of this graph. The values of  $\phi_B$  for different cells are given in Table 4.1.

#### b) Capacitance-Voltage characteristics in dark

The electrode/electrolyte interface can further be analysed to obtain the flat band potential by the measurement of space charge layer capacitance. It is the correlation between charge density and electrostatic potential at the interface. Since the electrostatic potential cannot be measured directly, the most valuable information can be obtained from the capacitance measurement of a space charge layer. Hence C-V measurement provides a convenient tool for obtaining the useful information about both semiconductor and an electrolyte. Thus the flat band potential  $V_{fb}$  is an important parameter for explaining the PEC properties of the system in dark and under illumination /2,9,24/. It is a measure of a potential which must be applied to the semiconductor such that bands remain flat at the interface. Therefore measurements have been made of the capacitance as a function of the applied bias in dark to deduce the flat band

potential,  $V_{fb}$ . Figure 4.13 shows the plots of  $C^{-2}$  vs  $V$  for four typical cells. The intercepts of the plots on the voltage axis give value of the flat band potential. They are shown in Table 4.1. From the figure 4.13 it seems that the variation of  $C^{-2}$  vs  $V$  deviates from the linearity, especially at high applied voltage levels. The non-linearity shows the graded type of junctions formed /9,17/ and is caused by; i) non-uniform a.c current distribution, ii) presence of the impurities, iii) ionic adsorption on the electrode surface and presence of the surface states /9,17,25/.

#### c) Power output characteristic in light

The photovoltaic output curves were obtained for all the cells under constant illumination intensity ( $40 \text{ mW/cm}^2$ ). When a PEC cell is irradiated it acts as generator of an electricity which is in accordance with the standard principles of the PEC cells /9,25,26/. The generation of a photovoltage and a photocurrent property of a photoelectrochemical cell can be understood from the equivalent circuit of a cell (figure 4.14). The photocurrent is represented by a current source. If the forward current, in dark, through the junction is  $I_d$  then series resistance of a cell can be represented by a fixed lumped resistance  $R_s$  which arises mainly from the bulk resistance of a material /9,17,25,27/. The back contact of the cell is considered to be ohmic and an electrolyte offers a negligible resistance to the flow of current. The shunting paths are provided through micropores and along the edges of the material and are shown as  $R_{sh}$  /9/.  $R_L$  is the load resistance to the cell and  $V_{oc}$  is the open circuit voltage obtainable from a cell. We consider the

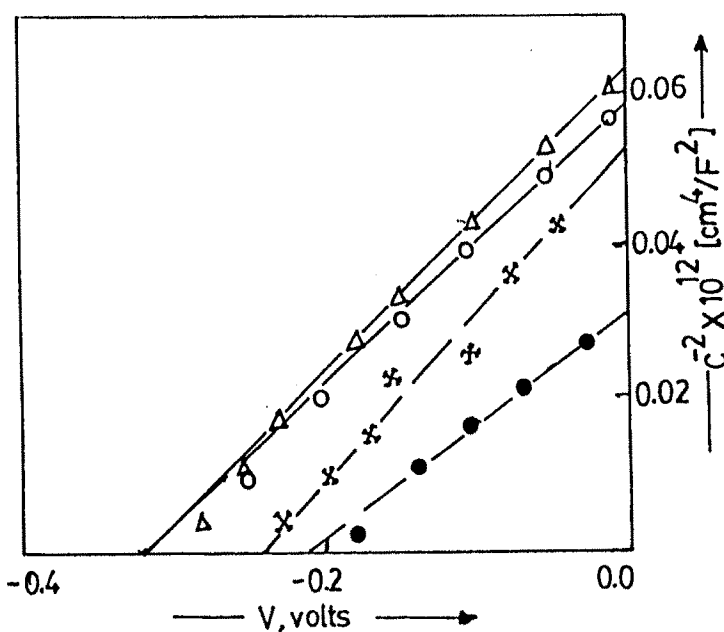


Fig.4.13 Mott - Schottky plots for four typical cells formed with photoelectrodes :  
 ● → Pure PbS, ○ → X = 0.05, Δ - X = 0.15 and \* → X = 0.5.

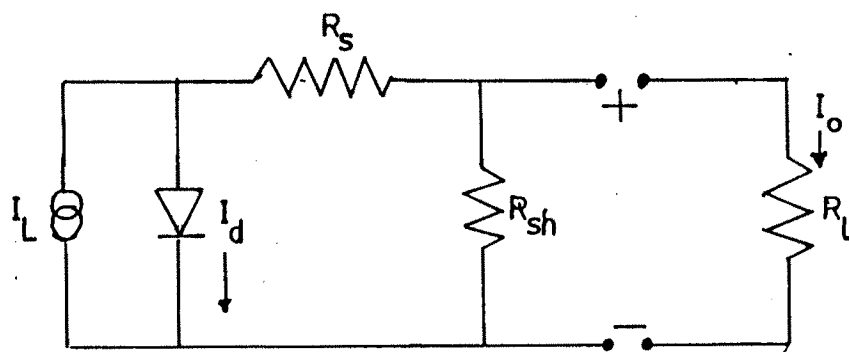


Fig.4.14 The equivalent circuit of PEC cell.

Schottky diode equation for the S/E interface and thus the photocurrent of a cell under illumination can be given as /9,19,24/;

$$I = I_L - I_d \frac{V_{oc}}{R_{sh}} \quad \dots(4.15)$$

$$I = I_L - I_o \left[ \exp \left( \frac{qV}{n_L KT} \right) - 1 \right] - \frac{V_{oc}}{R_{sh}} \quad \dots(4.16)$$

where,  $I_L$  is the photocurrent,  $I_d$  is the dark current,  $I_o$  is the reverse saturation current and  $V$  is the applied voltage. As  $R_{sh}$  for the cell is expected to be very high  $V_{oc}/R_{sh}$  is meaningless and equation (4.16) takes the form;

$$I = I_L - I_o \left[ \exp \left( \frac{qV}{n_L KT} \right) - 1 \right] \quad \dots(4.17)$$

For bias voltages exceeding  $3KT/q$  one can also neglect last term in equation (4.17). Moreover, at open circuit conditions,  $I_L = 0$  and  $V = V_{oc}$ , thus rearrangement of equation yields /9,17,24/;

$$V_{oc} = \frac{n_L KT}{q} \ln \frac{I_{sc}}{I_o} \quad \dots(4.18)$$

Under short circuit condition,  $V_{oc} = 0$  and

$$I = I_L - I_o \cong I_{sc} \quad \dots(4.19)$$

The power output curves are shown in figure 4.15 for five typical cells. The series resistance ( $R_s$ ) and shunt resistance ( $R_{sh}$ ) have been calculated for all the cell configurations. The fill factor (ff) and the energy conversion efficiency ( $\eta$ ) have been deduced from these curves and are listed in Table (4.1).

#### 4.4.2 Optical studies

The photo and speed responses have been studied for the typical cells.

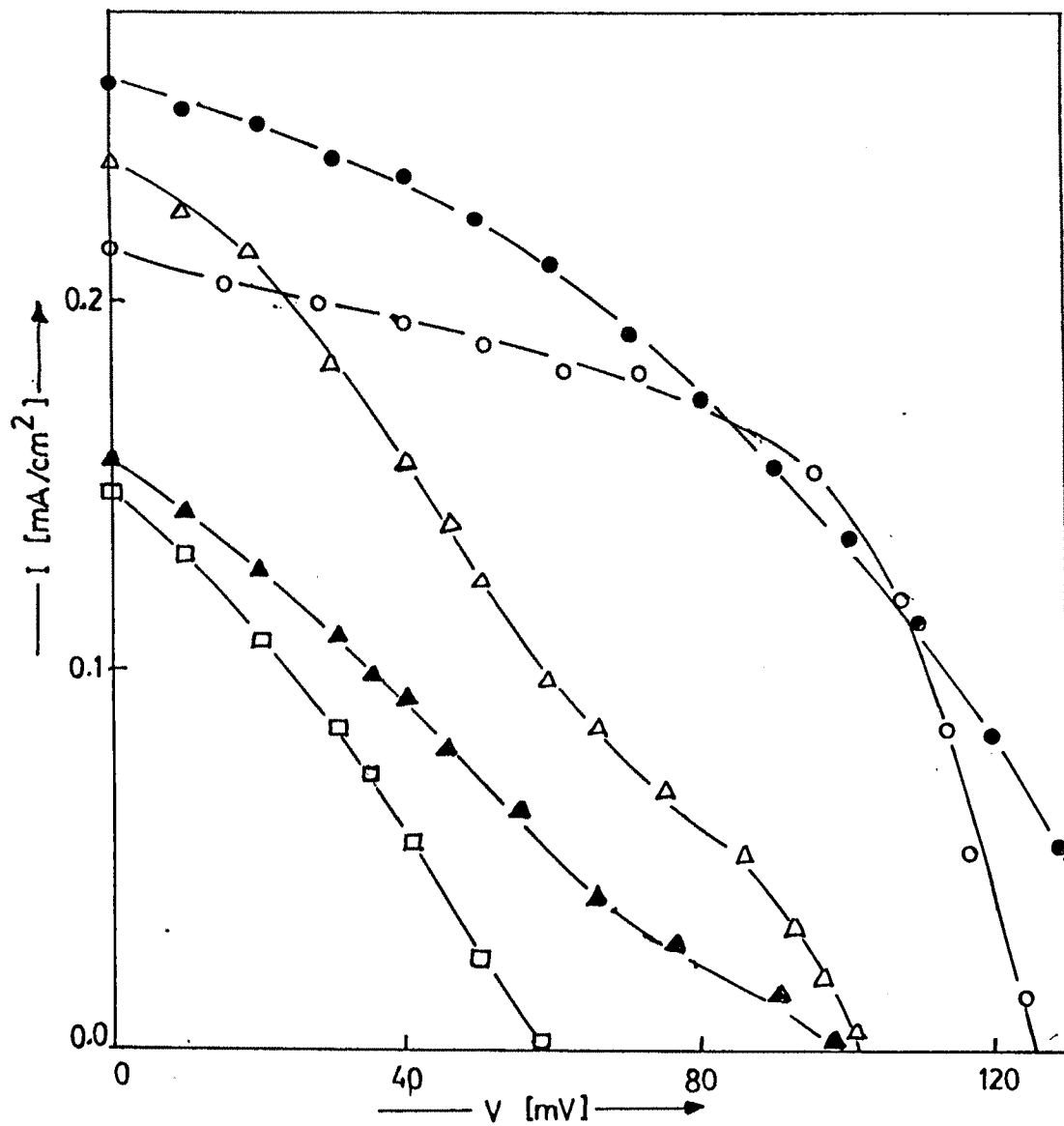


Fig.4.15 photovoltaic power out put curves for five typical cells.

□ → pure PbS, ● →  $X = 0.05$ , △ -  $X = 0.075$ ,  
 ○ →  $X = 0.15$ , ▲ →  $X = 0.35$ .

### a) Photo response

The short circuit current ( $I_{SC}$ ) and open circuit voltage ( $V_{OC}$ ) have been recorded at various illumination intensities. Their variation with input optical power is shown, for two typical cells in figure 4.16. It has been observed that  $I_{SC}$  varies almost straight for the whole range of input optical power obeying the relation /9/;

$$I_{SC} = C \cdot F_L \quad \dots(4.20)$$

where,  $C$  = constant, which depends on the fraction of the light utilised for generation of the carriers. The variation of  $V_{OC}$  with light intensity is initially faster and saturates for higher input intensities. The saturation of  $V_{OC}$  can be related to the presence of surface states and surface adsorbed ions at the interface /9,27/.

### b) Speed of response

Study of  $I_{SC}$  and  $V_{OC}$  with time is important to know the charge transfer mechanism at the semiconductor /electrolyte junction. Figure 4.17 shows  $V_{OC}$  rise and decay with time for the cell under light excitation. Relatively fast rise and slow decay is observed in the present study and can be related to the adsorption of the electrolyte molecules on the surface of the photoelectrode and dense population of the surface states at the interface /19,21,27/. It is not possible to determine the minority carrier life time by the  $V_{OC}$  decay technique as most of the role of charge transport is played by the ions in the electrolyte. The decay of the  $V_{OC}$  follows second order kinetics /9,19/ as:

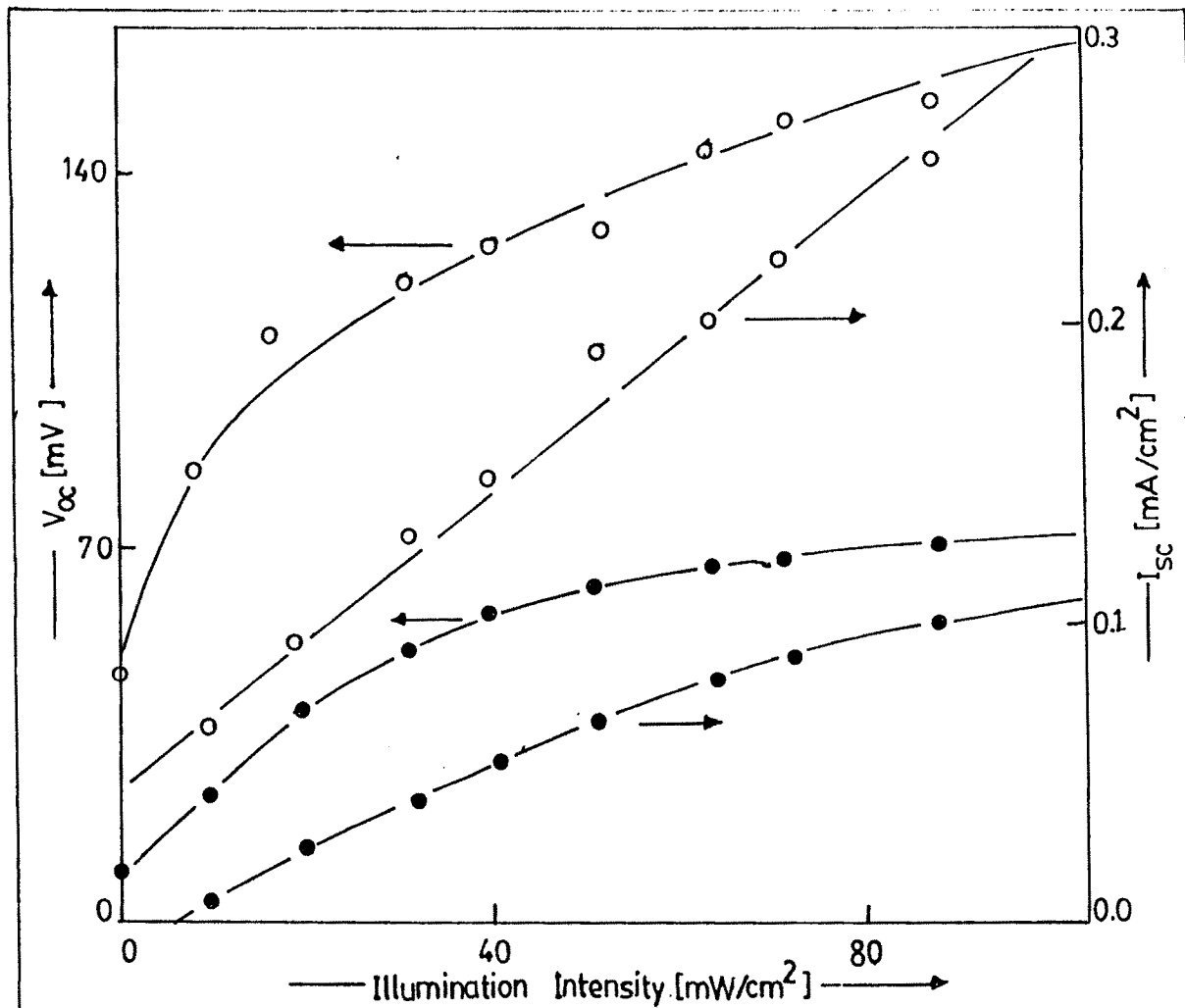


Fig.4.16 Variation of Voc and Isc with intensity of illumination. ● → Pure PbS and ○ → X = 0.05.

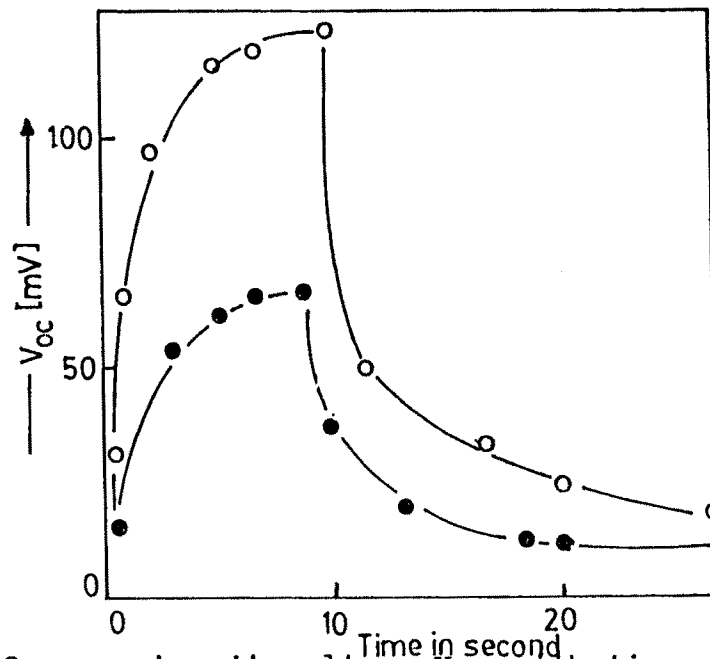


Fig.4.17 Variation of open circuit voltage Voc with time. ● → Pure PbS and ○ → X = 0.05.

$$V_{OC}(t) = V_{OC}(0)t^{-b} \quad \dots(4.21)$$

where,  $V_{OC}(0)$  and  $V_{OC}(t)$  are open circuit voltages at  $t = 0$  and  $t$  second, respectively and 'b' is a rate constant. Further, slow decay in  $V_{OC}$  can also be ascribed to pinning of the Fermi level under light excitation.

#### c) Spectral response

Although study of spectral response is important for PEC cells since it is directly related to the solar spectrum and provides useful informations for identifying the recombination centres and therefore diagnosing the problems related to the efficiency losses, we could not proceed for the same because of the wavelength limitations.

#### 4.5 Conclusions

A photoelectrochemical cell formed with PbS:CuS photoelectrode has an efficiency much lower than that of the expected. Incorporation of Cu in PbS has improved the solar cell performance by a very small amount (Table 4.1). However, at this moment, the results are not encouraging. The major reason is its high electrical resistivity. In order to improve the performance of PbS:CuS based PEC cells it is essential to reduce its electrical resistivity drastically by optimising various parameters and deposition conditions such as thickness, concentration, post preparative treatments, selection of a proper electrolyte etc. Attempts in this direction are under progress.

## REFERENCES

1. H.Gerischer, Z. Phys. Chem., 26(1960) 223
2. H.Gerischer , in " Physical Chemistery " An Advanced Treatise, (eds) H.Eyring , D. Henderson and W. Jost. Vol.94 (Academic Press, N.Y. ) 1970
3. H.Helmholtz, Wied, Ann 7 (1979) 337
4. A.Gouy, J. Physique 4(1990) 457
5. D.L.Chapman, Phil.Mag.(ser 6) 26 (1913) 475
6. J.O.M.Bockris and A.K.N. Reddy in "Modern Electrochemistry (eds) J.O.M.Bockris and A.K.N.Reddy, Vol-2,(Plenum press,N.Y.) 1973) 862
7. W.H.Brattain and G.B.Garret, Bell.Syst.Tech.,J.34(1955) 129
8. R.Memming, Phil. Tech. Rev., 38(1979)160
9. S. Chandra in "Photoelectrochemical Solar Cells ", (eds) D.S. Campbell (Gorden and Breach Science Publishers), N.Y, (U.S.A.) 1985
10. W.H.Lafler, F.Cardon and W.P.Gomes, Surface Sci.,44(1979) 541
11. E.C.Dutoit, F.Cardon and W.P.Gomes, Ber. Bunsenges Phys. Chem. 79(1975) 1205
12. J.H.Kenedy and K.W. Frese Jr.J.Electro-chem. Soc. , 125(1978) 709 and 125 (1978)723
13. H.Gerischer, J.Pure and Appl. Chem.,52(1980) 2449
14. H. Gerischer, in "Semiconductor Liquid Junction Solar Cells" (ed) A.Heller, The Electrochem Soc. Inc. Princerton , N.J. (1977) P.1
15. M.D.Archer , J.Appl.Electrochem.,5 (1975) 17
16. S.H.Pawar and L.P. Deshmukh , Mat. Cham. Phys., 10(1984)83

17. L.P. Deshmukh , A.B. Palwe and V.S. Sawant , Solar Cells, 28(1990)1
18. C.D.Lokhande and S.H. Pawar , Mat., Chem. Phys. , 11(1984)201
19. L.P.Deshmukh , Ph.D., Thesis Shivaji University , Kolhapur (1985) M.S. India
20. A. Heller, K.C. Chang and B.Miller , J Electrochem. Soc., 124(1977) 696
21. K. Rajeshwar, R.Thomson , P. Singh , R.C. Kainthala and K.L. Chopra , J. Electrochem. Soc., 128 (1981) 1177
22. M.A.Butler , J, Appl. Phys., 48(1977) 1914
23. D.S. Ginley and M.A. Butler , J. Appl. Phys., 48(1977) 2019
24. K.Rajeshwar , P.Singh and J. Dubow, Electrochemica Acta, 23 (1978)1117
25. L.P. Deshmukh , P.P. Hankare and V.S.Sawant, Solar Cells, 31 (1991)549
26. J.Reichman and M.A.Russak, in Photoeffects at Semiconductor -Electrolyte Interface, Ed. A.J.NOZIK, ACS Sym., 146(1981)359
27. F.El. Guibalaly and K. Colbow, Can. J. Phys., 59(1981) 1682